

Polaron formation for a non-local electron-phonon coupling: A variational wave-function study

C. A. Perroni,^{1,2} E. Piegari,² M. Capone,³ and V. Cataudella^{1,2}
¹*Coherentia-INFM, UdR di Napoli, via Cinthia 80126 Napoli (Na), Italy*
²*Dipartimento di Fisica, Università di Napoli "Federico II", Italy*
³*Enrico Fermi Center, Rome, Italy*
 (March 13, 2021)

We introduce a variational wave-function to study the polaron formation when the electronic transfer integral depends on the relative displacement between nearest-neighbor sites giving rise to a non-local electron-phonon coupling with optical phonon modes. We characterize the polaron crossover by analysing ground state properties such as the energy, the electron-lattice correlation function, the average phonon occupation and the quasiparticle spectral weight. Variational results are found in good agreement with numerical exact diagonalization of small clusters, and follow the correct perturbative result at weak coupling. We determine the polaronic phase diagram and we find that the tendency towards strong localization is hindered from the pathological sign change of the effective next-nearest-neighbor hopping.

I. INTRODUCTION

Significant electron-phonon (el-ph) interactions have been experimentally detected in many materials of wide interest, like manganites,¹ fullerenes,² carbon nanotubes,^{3,4} and cuprates.⁵ In many of these cases, the el-ph interaction gives rise to polaronic features. A polaronic state results in fact when the electrons are strongly coupled to lattice distortion, therefore increasing their effective mass and leading to a state with low mobility. Increasing the el-ph coupling, the spatial extension of the lattice deformation decreases⁶ and the polaron can vary its size from *large* to *small*. The single polaron problem of one electron interacting with the lattice degrees of freedom has been studied in detail, and allowed us to understand in the detail the physics leading to the formation of polaronic states. In particular it has been shown that the self-trapping process, which lead to the formation of polarons, is not a phase transition, but just a continuous crossover with no broken symmetry.⁷ In the case of the Holstein model,⁸ where quantum vibrations interact *locally* with the electrons, the crossover from large to small polaron has been extensively studied by several numerical techniques^{9–15} and variational approaches.^{16–18} In particular all the ground state properties of the Holstein model can be described with great accuracy by a variational approach¹⁸ based on a linear superposition of Bloch states that describe weak and strong coupling polaron wave functions.

The case of non-local interactions, that in general are also present in real materials, is much less understood. The coupling with acoustical phonons has been studied in order to explain the anomalous transport properties of non-local excitations, like solitons and polarons, in various 1D systems.^{19–22} In particular the tight-binding Su-Schrieffer-Heeger (SSH) model¹⁹ was introduced to explain the transport properties of quasi one-dimensional polymers as polyacetylene where the CH monomers form chains of alternating double and single bonds. In this case the localization is due to a large shrink of two particular bonds and corresponding large hopping integral between the sites. As a result, the hopping between the two occupied sites and the surrounding ones is reduced resulting in a tendency towards localization.

Our purpose here is to examine the single polaron formation in a model where both (Holstein) local and (SSH) non-local el-ph interactions are present. Due to the complexity of the model, we start the analysis using a perturbative approach that, although it can not capture the full multiphononic nature of the polaron, it has proved a remarkably useful tool in understanding the el-ph physics.^{12,22} In particular we characterize the ground state properties of the system evaluating the energy, the electron-lattice correlation function and the quasiparticle spectral weight, in order to provide signatures of the polaron formation. In the limit when local el-ph interactions are much stronger or weaker than non-local el-ph interactions our model reduces to the standard Holstein model and to the SSH model with a dispersionless phonon spectrum, respectively. Then we start an accurate analysis of the non-local limit case, being this case not yet fully examined. Recently, the fully adiabatic regime of this model has been used to explain changes in carbon-nanotube length as a function of charge injection.⁴ Furthermore the non-local case has been previously studied by one of us using exact diagonalization of small clusters up to four lattice sites, where an anomalous optical absorption has been identified.¹² In particular in Ref. [12] it is shown that the strong-coupling solution is characterized by an

unphysical sign change of the effective next-nearest-neighbor hopping which is missing when acoustical phonons are considered.²¹

In this work we improve the previous numerical analysis considering a six-site lattice and introduce a variational wave-function to investigate the thermodynamic limit of the system. The variational approach is based on a linear superposition of Bloch states that provide an excellent description of the lattice deformations on left and right bond of the polaron, respectively. The wave-function closely resembles a variational state previously proposed for the study of the Holstein model¹⁸ and for the SSH case it allows to describe polaron features in good agreement with exact numerical diagonalization results. The variational approach recovers the pathological behavior of the effective next-nearest-neighbor hopping pointing out that the non-physical region of parameters always prevents a strong localized solution. We also explicitly show that, when the phonon frequency is not really small, the considered non-local SSH interaction supplies a tendency to localize for the single carrier which can be more effective than the Holstein localization.

The scheme of the paper is the following. In Sec. II we present the model and set down the notation. In Sec. III we discuss perturbative calculations showing the role of SSH el-ph coupling with respect to the Holstein contribution. Sec. IV is devoted to the presentation of the variational method in the limit of non-local el-ph interactions and its comparison with the exact diagonalization results. Sec. V reports our concluding remarks.

II. THE MODEL

In extremely general terms, the interaction between electron and harmonic lattice deformations is described by the Hamiltonian

$$\mathcal{H} = \sum_{i,j,\sigma} c_{i,\sigma}^\dagger t_{i,j}(\{x_k\}) c_{j,\sigma} + \sum_i \frac{p_i^2}{2M} + \sum_{i,j} \frac{x_i K_{i,j} x_j}{2} + \sum_{i,\sigma} e_i(\{x_k\}) c_{i,\sigma}^\dagger c_{i,\sigma}, \quad (1)$$

where $c_{i,\sigma}^\dagger$ ($c_{i,\sigma}$) is the fermion creation (destruction) operator, σ is the spin index, $t_{i,j}(\{x_k\})$ is the electronic transfer integral for fixed lattice deformations $\{x_k\}$, M is the ionic mass, $K_{i,j}$ is the spring constant matrix, and $e_i(\{x_k\})$ is the local energy of the electron. For small deviations from the equilibrium positions of the lattice we can approximate $t_{i,j}(\{x_k\})$ and $e_i(\{x_k\})$ to be linear functions of the lattice displacements $\{x_k\}$ obtaining a general model with el-ph interactions. In particular, limiting the hopping to nearest-neighbor sites of a linear chain, we make the assumption

$$t_{n+1,n}(\{x_k\}) = -t + \alpha(x_{n+1} - x_n) \quad (2)$$

typically employed for the derivation of the el-ph SSH interaction term, and

$$e_i(\{x_k\}) = \alpha_1 x_i \quad (3)$$

generally used in order to deduce the local el-ph Holstein interaction. If spinless electrons and dispersionless Einstein phonons are considered, the model becomes

$$\mathcal{H} = -t \sum_i (c_i^\dagger c_{i+1} + c_{i+1}^\dagger c_i) + \omega_0 \sum_i a_i^\dagger a_i + H_{int}, \quad (4)$$

where H_{int} is

$$H_{int} = g\omega_0 \sum_i (c_i^\dagger c_{i+1} + c_{i+1}^\dagger c_i)(a_{i+1}^\dagger + a_{i+1} - a_i^\dagger - a_i) + g_1\omega_0 \sum_i c_i^\dagger c_i(a_i^\dagger + a_i), \quad (5)$$

with a_i^\dagger (a_i) the phonon creation (destruction) operator and ω_0 the quantum of vibrational energy per site. The quantity $g = \alpha/\sqrt{2M\omega_0^3}$ is the SSH coupling that we mainly discuss in this work, while $g_1 = \alpha_1/\sqrt{2M\omega_0^3}$ is the Holstein local electron-phonon coupling. We study the coupling of a single electron to lattice deformations using units such that the lattice spacing $a = 1$ and $\hbar = 1$.

III. PERTURBATION THEORY

Weak-coupling perturbation theory in the electron-phonon coupling has proved a remarkably useful tool in understanding the el-ph physics. Besides the obvious ability to describe the weakly interacting regime, the perturbative

approach has in fact provided some guidelines to understand the conditions for polaron formation in the Holstein model. More explicitly, the polaron crossover occurs around the coupling value for which the perturbative approach breaks down.¹²

Here we focus on the case of one electron in a one-dimensional chain. If the el-ph terms are smaller than both the hopping term and the bare phonon term ($g, g_1 \ll \tilde{t}, 1$ and $\tilde{t} = t/\omega_0$), they can be treated as perturbations of the unperturbed Hamiltonian $H_0 = H_{kin} + H_{ph}$.

The second-order correction to the energy of the ground state is given by

$$\Delta E(0) = -g^2 \left(\frac{1 + 2\tilde{t} - \sqrt{1 + 4\tilde{t}}}{\tilde{t}^2} \right) - g_1^2 \frac{1}{\sqrt{1 + 4\tilde{t}}}, \quad (6)$$

while the perturbative correction to the free band $\varepsilon_k = -2t \cos(k)$ is reported in Appendix A.

We note that for fixed values of the coupling constants g and g_1 the two contributions (SSH-like and Holstein) have different behaviors as functions of the inverse adiabatic ratio \tilde{t} . In particular, as shown in Fig. 1, the Holstein contribution to the ground state energy is always lower (for $g = g_1$) than the SSH one when $\tilde{t} < \tilde{t}_w$ with $\tilde{t}_w = 4 + 3\sqrt{2}$. In other words, when the phonon frequency are not really small, the SSH el-ph coupling is more effective than the Holstein one. The reduced effect of the Holstein el-ph coupling when \tilde{t} is small (anti-adiabatic regime) pushes the polaron crossover to larger values of the coupling $\lambda = g^2/2\omega_0 t$ as the phonon frequency is increased. Actually, while $\lambda > 1$ is the condition for the polaron crossover in the adiabatic regime $\tilde{t} \gg 1$, in the antiadiabatic regime $\tilde{t} \ll 1$, it has been shown that the crossover occurs when $\alpha^2 = g^2/\omega_0^2 \simeq 1$, i.e., for $\lambda \gg 1$.^{12,14,15} Recently it has been shown that this important role of the degree of adiabaticity is not limited to the single polaron problem, but it also extends to finite densities.²³

Since polaron formation is not a phase transition and occurs without symmetry breaking, different criteria can be established to define the crossover values of the coupling constants which mark the polaronic regime. In the following we compute some physical quantities which have been often introduced to characterize the polaron crossover.

The average phonon occupation number $N_{ph} = \frac{1}{N} \langle \sum_i a_i^\dagger a_i \rangle$ is given by

$$N_{ph} = \frac{2\lambda}{\tilde{t}} \left[\frac{(1 + 2\tilde{t})}{\sqrt{1 + 4\tilde{t}}} - 1 \right] + 2\lambda_1 \tilde{t} \frac{(1 + 2\tilde{t})}{(1 + 4\tilde{t})^{3/2}}, \quad (7)$$

where $\lambda = g^2\omega_0/2t$ and $\lambda_1 = g_1^2\omega_0/2t$. From Eq. (7) it turns out that the phonon number, as the ground state energy, is more affected by the SSH coupling when ω_0 exceeds a given value. In particular for $\tilde{t} \leq 2$ (i.e. $\omega_0/t \geq 0.5$) the SSH contribution is always higher than the Holstein one.

Other quantities of great interest to characterize the polaron formation are the electron-lattice correlation functions. In particular we consider the correlation function $\chi_{i,\delta} = \langle c_i^\dagger c_i (a_{i+\delta}^\dagger + a_{i+\delta}) \rangle$ between the electronic density on a site i and the lattice displacement on site $i + \delta$, which measures the entanglement of lattice and electronic degrees of freedom typical of the polaronic state. After a Fourier transformation in the momentum space, at $k = 0$ one has

$$\begin{aligned} \chi_{k=0,\delta=0} &= -\frac{2g_1}{\sqrt{1 + 4\tilde{t}}} \\ \chi_{k=0,\delta=1} &= -\frac{g}{\tilde{t}^2} (1 + 2\tilde{t} - \sqrt{1 + 4\tilde{t}}) - \frac{g_1}{\tilde{t}} \left(\frac{2\tilde{t} + 1}{\sqrt{1 + 4\tilde{t}}} - 1 \right) \\ \chi_{k=0,\delta=2} &= -2g \left[\frac{1}{\tilde{t}} + \frac{1 + 4\tilde{t}}{2\tilde{t}^3} \left(1 - \frac{1 + 2\tilde{t}}{\sqrt{1 + 4\tilde{t}}} \right) \right] - 2g_1 \left[\frac{1}{\sqrt{1 + 4\tilde{t}}} + \frac{1 + 2\tilde{t}}{2\tilde{t}^2} \left(1 - \frac{1 + 2\tilde{t}}{\sqrt{1 + 4\tilde{t}}} \right) \right]. \end{aligned} \quad (8)$$

In Fig. 2 we plot the correlation function at nearest-neighbor (left) and next-nearest-neighbor (right) sites as functions of the inverse adiabatic ratio \tilde{t} , for fixed values of the couplings $g = g_1 = 1$. As expected, the value of the correlation function goes to zero for large values of \tilde{t} , but the behavior of the SSH-like contribution (dashed lines) is qualitatively different from that of the Holstein ones (dot-dashed lines).

The last quantity we consider is the quasiparticle spectral weight $Z(k) = (1 - \frac{\partial \Sigma(k, \omega)}{\partial \omega}|_{\omega=\varepsilon(k)})^{-1}$, which measures the renormalization of the electron Green's function due to the el-ph interaction. The second-order perturbative self-energy $\Sigma(k, \omega)$ is given in Appendix A. Even if the polaronic regime cannot be attained within lowest-order perturbative approach, indications on the beginning of the polaronic crossover can be extracted from the spectral weight expression. In particular the polaron crossover is expected to be associated with a sharp reduction of this quantity as a function of the couplings. The expression of the inverse spectral weight at $k = 0$ is given by

$$Z(0)^{-1} = 1 - \frac{2\lambda}{\tilde{t}} \left[1 - \frac{(1 + 2\tilde{t})}{\sqrt{1 + 4\tilde{t}}} \right] + 2\lambda_1 \tilde{t} \frac{(1 + 2\tilde{t})}{(1 + 4\tilde{t})^{3/2}}, \quad (9)$$

while the full momentum dependence of $Z(k)$ is reported in Appendix A. As expected the spectral weight $Z(0)$ is a monotonically increasing function of \tilde{t} , for a fixed value of the couplings. It is interesting to note that the reduction of $Z(0)$ due to the SSH-like contribution is more relevant of the Holstein ones for $\tilde{t} < 2$, while in the adiabatic limit, i.e. for large value of \tilde{t} , it is very small and slow.

Strictly speaking, perturbative calculations only correctly characterize the small coupling regime. In order to provide a better insight on the problem of the polaron formation in the systems with non-local interactions, in the following we focus on the SSH contribution and substantiate our results by analytic variational calculations and numerical exact data.

IV. VARIATIONAL APPROACH VS. EXACT DIAGONALIZATION

In this section we extend our analysis of the non-local SSH model to the whole range of el-ph couplings using two standard and well grounded techniques, a variational approach and exact diagonalization of small clusters. First we introduce the variational wave function. We consider translation-invariant Bloch states obtained by superposition of localized states centered on different lattice sites.²⁴ These wave-functions have been introduced in order to study the polaron formation within the Holstein model where they are able to fully capture the features of the Holstein polaron.^{16,18} In this work we extend this kind of wave-functions to the SSH interaction model assuming

$$|\psi_k^{(i)}\rangle = \frac{1}{\sqrt{N}} \sum_n e^{ik \cdot n} |\psi_k^{(i)}(n)\rangle, \quad (10)$$

where $|\psi_k^{(i)}(n)\rangle$ is defined as

$$|\psi_k^{(i)}(n)\rangle = e^{[U_k^{(i)}(n) + U_k^{(i)}(n-1) + U_k^{(i)}(n+1)]} |0\rangle_{ph} \sum_m \phi_k^{(i)}(m) e^{ik \cdot m} c_{n+m}^\dagger |0\rangle_{el}, \quad (11)$$

with the quantity $U_k^{(i)}(j)$ given by

$$U_k^{(i)}(j) = \frac{g}{\sqrt{N}} \sum_q [f_{k,j}^{(i)}(q) a_q e^{iq \cdot R_j} - h.c.]. \quad (12)$$

The phonon distribution function $f_{k,j}^{(i)}(q)$ is chosen as

$$f_{k,j}^{(i)}(q) = \frac{\alpha_{k,j}^{(i)}}{1 + 2\tilde{t}\beta_{k,j}^{(i)} [\cos(k) - \cos(k+q)]}, \quad (13)$$

with $\alpha_{k,j}^{(i)}$ and $\beta_{k,j}^{(i)}$ variational parameters. In Eq. (11), $|0\rangle_{ph}$ and $|0\rangle_{el}$ denote the phonon and electron vacuum state, respectively, and the variational functions $\phi_k^{(i)}(m)$ are assumed to be

$$\phi_k^{(i)}(m) = \sum_{j=-5}^5 \gamma_k^{(i)}(j) \delta_{m,j}, \quad (14)$$

where $\gamma_k^{(i)}(j)$ are variational parameters that take into account the broadening of the electron wave-function up to fifth neighbors. It is worth to note that traditional variational approaches to the Holstein polaron problem uses the localized state (11) where only the on-site operator $U_k^{(i)}(n)$ is applied. Thus we introduce in the expression of the trial wave-function the nearest-neighbor displacement operators $U_k^{(i)}(n+1)$ and $U_k^{(i)}(n-1)$, in order to take into account the dependence of the hopping integral on the relative distance between two adjacent ions.

Reflecting the asymmetry of the SSH coupling (shrinking of the bond on which the electron is localized and stretching of the neighboring bonds), we also define two wave-functions that provide a very good description of the lattice deformations on left and right bonds of the polaron. Naturally the left and right directions are relative to the site

where the presence of the electron is more probable. Thus in Eq. (11) the apex $i = L, R$ indicates the *Left* (L) and *Right* (R) polaron wave-function, respectively. The wave-functions L and R are related as follows

$$\begin{aligned} f_{k,n}^{(R)}(q) &= -f_{k,n}^{(L)}(q) < 0 \\ f_{k,n-1}^{(R)}(q) &= -f_{k,n-1}^{(L)}(q) > 0 \\ f_{k,n+1}^{(R)}(q) &= -f_{k,n+1}^{(L)}(q) > 0 \\ \phi_k^{(R)}(m) &= \phi_k^{(L)}(-m). \end{aligned} \quad (15)$$

All the variational parameters are determined by minimizing the expectation value of the Hamiltonian (4) with $g_1 = 0$ on the states (11). Even though the wave-functions L and R describe correctly the lattice deformations of the left and right side of the polaron, respectively, the mean values of the Hamiltonian on these states are equal. So the relations (15) can be also viewed as those that leave unchanged the energy functional determined by one wave-function.

These two wave-functions can be improved by increasing the extension of the phonon contributions in Eq. (11) and of the electron terms in Eq. (14). Furthermore, they are not orthogonal and the off-diagonal matrix elements of the Hamiltonian between these two states are not zero. This allows to determine the ground-state energy by considering as trial state the linear superposition¹⁸ of the wave-functions R and L

$$|\psi_k\rangle = \frac{A_k|\Phi_k^{(R)}\rangle + B_k|\Phi_k^{(L)}\rangle}{\sqrt{A_k^2 + B_k^2 + 2A_kB_kS_k}}, \quad (16)$$

where $|\Phi_k^{(L)}\rangle$ and $|\Phi_k^{(R)}\rangle$ are the normalized wave-functions L and R weighted by the coefficients A_k and B_k and

$$S_k = \langle\Phi_k^{(L)}|\Phi_k^{(R)}\rangle \quad (17)$$

is the overlap factor. The wave-function (16) correctly describes the properties of the lattice deformations on both the sides of the polaron and we will find that it is in very good agreement with the results derived by the exact diagonalizations on a chain of 6 sites. Furthermore the variational approach involves a number of variational parameters that does not depend on the length of chain, so it allows to study the thermodynamic limit of the system.

The minimization procedure is performed in two steps. First the energies of the left and right wave-functions are separately minimized, then these wave-functions are used in the minimization procedure of the quantity $E_k = \langle\psi_k|H|\psi_k\rangle/\langle\psi_k|\psi_k\rangle$ with respect to A_k and B_k defined in (16).¹⁸ Exploiting the equality

$$\langle\psi_k^{(L)}|H|\psi_k^{(L)}\rangle = \langle\psi_k^{(R)}|H|\psi_k^{(R)}\rangle = \varepsilon_k, \quad (18)$$

we obtain

$$E_k = \frac{\varepsilon_k - S_k E_{kc} - |E_{kc} - S_k \varepsilon_k|}{1 - S_k^2}, \quad (19)$$

where $E_{kc} = \langle\Phi_k^{(L)}|H|\Phi_k^{(R)}\rangle$ is the off-diagonal matrix element, and $|A_k| = |B_k|$. The matrix elements between the states $\psi_k^{(R)}$ and $\psi_k^{(L)}$ contained in Eq. (19) are reported in Appendix B.

The total energy functional (19) is minimized with respect to the variational parameters and the optimal ground state energy is plotted in Fig. 3 for a six-site lattice and two different values of the inverse adiabatic parameter \tilde{t} . We also study the thermodynamic limit and find energy curves very close to those of the finite system. In order to test the validity of our variational approach (VA), we perform exact numerical calculations on small clusters by means of the Lanczos algorithm. We improve the previous exact diagonalization (ED) analysis of the model, investigating small clusters up to six sites.¹² As shown in Fig. 3, each variational and exact numerical curve exhibits a kink with increasing the el-ph coupling. We have checked that at these couplings the effective next-nearest-neighbor hopping changes sign opening an unphysical region of the parameters. The agreement between numerical data and variational approach is very good up to g values close to the unphysical transition.

In order to characterize the polaron formation we also analyze the electron-lattice correlation function $\chi_{i,\delta}$ defined in Sec. III. In particular in Fig. 4 we show the behavior of $\chi_{i,\delta}$ as a function of the SSH coupling for $\delta = 0, 1, 2$ and $\tilde{t} = 2.5$. As expected, variational results and exact numerical data always recover the perturbative values in the limit of small el-ph coupling. Increasing g the monotonic behavior of the correlation function exhibits a kink, as the ground state energy. In particular the correlation function at next-nearest-neighbor ($\delta = 2$) changes sign as the effective hopping, confirming the pathological behavior. At couplings where the ground state energy and the

correlation function show the kink, also the average phonon number is characterized by an anomalous behavior as shown in the bottom right panel of Fig. 4.

In order to extract information on the values of g at which polaron crossover begins, before the opening of the unphysical region, we also investigate the behavior of the quasiparticle spectral weight $Z(0)$. We find that increasing the el-ph coupling for fixed values of \tilde{t} , the spectral weight starts to drop but it never reaches a really small value before the unphysical sign change of the hopping occurs. Nevertheless we observe distinct signatures of the tendency towards localization, as shown in Fig. 5, where $Z(0)$ is plotted as a function of g for the fixed value $\tilde{t} = 2.5$.

We conclude our analysis collecting the obtained data in the phase diagram of Fig. 6. It is calculated from the position of the kink in the ground state energy obtained by means of the variational approach (diamonds) and the exact diagonalization (triangles). The agreement between the two methods becomes better moving towards the adiabatic limit. In analogy with the phase diagram obtained for the Holstein polaron,¹⁸ we also mark a crossover region defined as the range of parameters for which $Z(0)$ is less than 0.9. As shown in Fig. 6, we find that the considered SSH model does not present any marked mixing of electronic and phononic degrees of freedom, being the strongly coupled state prevented from the pathology of the model. As far as the fully adiabatic limit $\omega_0 = 0$ is concerned, we verify that the crossover line joins onto the line for the transition to the unphysical region at the critical value $\lambda = 0.25$, confirming the discussion in Ref. [12]. We finally notice that, as discussed in Ref. [12], both the crossover region boundary, and the instability line obtained by exact diagonalization are only weakly dependent on the adiabatic ratio, and that λ is the relevant electron-phonon coupling regardless the value of \tilde{t} . This is a peculiarity of the SSH coupling with respect to the Holstein one, where the polaron crossover moves to large values of λ as the phonon frequency increases.^{12,14,15,23}

V. CONCLUSIONS

In this work we discussed the features of one electron non-locally interacting with optical phonons in a discrete chain. We introduced a variational wave function to locate the crossover region for the transition between weak and strong localized polaron solutions. In particular we found that the pathological sign change of the effective next-nearest-neighbor hopping always precedes a stable strongly localized solution. Such an unphysical region of the model parameters does not occur in the case of acoustical phonons being the deformation linked to the particle extension along the entire chain.²¹ However we have also shown that, for finite values of the adiabaticity parameter, when the phonon frequency is not really small, the non local (SSH) el-ph interaction is more effective than the local (Holstein) one in reducing the mobility of the electron. Then our variational calculations are an interesting starting point to examine the complex problem of the polaron formation in a model where both local and non-local el-ph interactions are present. In particular we emphasize that the proposed variational wave function for the SSH limit can be slightly modified to be suitable for the treatment of the complex case where both interactions are present. Detailed future investigations in this direction are required. Finally we stress that the validity of our variational results is supported by an accurate analysis of exact diagonalization data on small clusters. The agreement between VA and ED data is good up to coupling values close to the unphysical region.

VI. ACKNOWLEDGEMENTS

M. C. acknowledges the hospitality and financial support of the Physics Department of the University of Rome "La Sapienza", as well as the INFM, UdR Roma 1 and SMC, and Miur Cofin 2001.

APPENDIX A

In the limit of small el-ph couplings, the perturbative second order correction $\Delta E(k)$ to the tight-binding free band energy is

$$\Delta E(k) = -4g^2\omega_0 \left[\frac{1 + 2\tilde{t}\cos k}{4\tilde{t}^2} + \frac{\sin^2 k}{\sqrt{1 + 4\tilde{t}\cos k - 4\tilde{t}^2(1 - \cos^2 k)}} - \frac{\sqrt{1 + 4\tilde{t}\cos k - 4\tilde{t}^2(1 - \cos^2 k)}}{4\tilde{t}^2} \right] - g_1^2\omega_0 \frac{1}{\sqrt{1 + 4\tilde{t}\cos k - 4\tilde{t}^2(1 - \cos^2 k)}}. \quad (20)$$

Moreover, using the bare phonon and electronic Green propagators, the perturbative self-energy reads

$$\Sigma(k, \omega) = \frac{4g^2\omega_0}{N} \sum_q \frac{[\sin(k+q) - \sin k]^2}{\omega - \omega_0 - \varepsilon(k+q) + i\delta} + \frac{g_1^2\omega_0}{N} \sum_q \frac{1}{\omega - \omega_0 - \varepsilon(k+q) + i\delta}. \quad (21)$$

From Eq. (21) we obtain the momentum dependent spectral weight

$$Z(k)^{-1} = 1 - \frac{2\lambda}{\tilde{t}} \left[1 - \frac{4\tilde{t}^2 \sin^2 k (1 + 2\tilde{t} \cos k)}{(1 + 4\tilde{t} - 4\tilde{t}^2(1 - \cos^2 k))^{3/2}} - \frac{(1 + 2\tilde{t} \cos k)}{\sqrt{1 + 4\tilde{t} - 4\tilde{t}^2(1 - \cos^2 k)}} \right] + 2\lambda_1 \tilde{t} \frac{(1 + 2\tilde{t} \cos k)}{(1 + 4\tilde{t} - 4\tilde{t}^2(1 - \cos^2 k))^{3/2}}. \quad (22)$$

APPENDIX B

In this appendix we report the matrix elements between the states $|\psi_k^{(R)}\rangle$ and $|\psi_k^{(L)}\rangle$. These quantities are involved in the calculation of the ground-state energy within the variational approach. We find

$$\langle \psi_k^{(L)} | \psi_k^{(R)} \rangle = \sum_{m_1, m_2} \phi_k^{*(R)}(-m_1) \phi_k^{(R)}(m_2) Z_k^{(L-R)}(m_1 - m_2), \quad (23)$$

where the phonon matrix element $Z_k^{(L-R)}(i-j)$ is defined as

$$Z_k^{(L-R)}(i-j) = {}_{ph} \langle 0 | e^{-[U_k^{(L)}(j) + U_k^{(L)}(j-1) + U_k^{(L)}(j+1)]} e^{-[U_k^{(R)}(i) + U_k^{(R)}(i-1) + U_k^{(R)}(i+1)]} | 0 \rangle_{ph}. \quad (24)$$

Then we have

$$\begin{aligned} \langle \psi_k^{(L)} | H_{kin} | \psi_k^{(R)} \rangle &= -t \sum_{m_1, m_2} \phi_k^{*(L)}(m_1) \phi_k^{(R)}(m_2) [e^{ik} Z_k^{(L-R)}(m_1 - m_2 + 1) e^{-ik} Z_k^{(L-R)}(m_1 - m_2 - 1)], \\ \langle \psi_k^{(L)} | H_{ph} | \psi_k^{(R)} \rangle &= -\omega_0 \sum_q \sum_{m_1, m_2} \phi_k^{*(L)}(m_1) \phi_k^{(R)}(m_2) [w_q^*(k)]^2 Z_k^{(L-R)}(m_1 - m_2) e^{iq(m_1 - m_2)}, \end{aligned} \quad (25)$$

and

$$\langle \psi_k^{(L)} | H_{int} | \psi_k^{(R)} \rangle = A_1 + A_2, \quad (26)$$

with A_1 and A_2 given by

$$\begin{aligned} A_1 &= \frac{g\omega_0}{\sqrt{N}} \sum_{q, m_1, m_2} \phi_k^{*(L)}(m_1) \phi_k^{(R)}(m_2) w_q^*(k) e^{ik} Z_k^{(L-R)}(m_1 - m_2 + 1) \left[e^{iq(m_2-1)} (1 - e^{iq}) + e^{-iqm_1} (e^{-iq} - 1) \right] \\ A_2 &= \frac{g\omega_0}{\sqrt{N}} \sum_{q, m_1, m_2} \phi_k^{*(L)}(m_1) \phi_k^{(R)}(m_2) w_q^*(k) e^{-ik} Z_k^{(L-R)}(m_1 - m_2 - 1) \left[e^{iqm_2} (1 - e^{iq}) + e^{-iq(m_1-1)} (e^{-iq} - 1) \right]. \end{aligned} \quad (27)$$

The quantity $\varepsilon_k = \langle \psi_k^{(L)} | H | \psi_k^{(L)} \rangle = \langle \psi_k^{(R)} | H | \psi_k^{(R)} \rangle$ is easily derived using the matrix elements given above.

¹ J. M. De Teresa, M. R. Ibarra, P. A. Algarabel, C. Ritter, C. Marquina, J. Blasco, J. Garcia, A. del Moral, and Z. Arnold, Nature **386**, 256 (1997); A. J. Millis, *ibid.* **392**, 147 (1998); M. B. Salamon and M. Jaime, Rev. Mod. Phys. **73**, 583 (2001).

² M. Matus, H. Kuzmany, and E. Sohmen, Phys. Rev. Lett. **68**, 2822 (1992); K. Harigaya, Phys. Rev. B **45**, 13676 (1992); B. Friedman, *ibid.* **45**, 1454 (1992); W. M. You, C. L. Wang, F. C. Zhang, and Z. B. Su, *ibid.* **47**, 4765 (1993).

- ³ M. Verissimo-Alves, R. B. Capaz, B. Koiller, E. Artacho, and H. Chacham, Phys. Rev. Lett. **86**, 3372 (2001); E. Piegari, V. Cataudella, V. Marigliano Ramaglia, and G. Iadonisi *ibid.* **89**, 049701 (2002); L. M. Woods and G. D. Mahan, Phys. Rev. B **61**, 10651 (2000); H. Suzura and T. Ando, *ibid.* **65**, 235412 (2002).
- ⁴ Yu N. Gartstein, A. A. Zakhidov, and R. H. Baughman, Phys. Rev. Lett. **89**, 045503 (2002).
- ⁵ Guo-Meng-Zhao, M. B. Hunt, H. Keller, and K. A. Muller, Nature **385**, 236 (1997); A. Lanzara, P. V. Bogdanov, X. J. Zhou, S. A. Kellar, D. L. Feng, E. D. Lu, T. Yoshida, H. Eisaki, A. Fujimori, K. Kishio, J.-I. Shimoyama, T. Noda, S. Uchida, Z. Hussain, and Z.-X. Shen, *ibid.* **412**, 510 (2001); R. J. McQueeney, J. L. Sarrao, P. G. Pagliuso, P. W. Stephens, and R. Osborn, Phys. Rev. Lett. **87**, 77001 (2001).
- ⁶ A. S. Alexandrov, N. F. Mott, Rep. Prog. Phys. **57**, 1197 (1994).
- ⁷ B. Gerlach and H. Lowen, Phys. Rev. B **35**, 4291 (1987); **35**, 4297 (1987).
- ⁸ T. Holstein, Ann. Phys. **8**, 325 (1959); **8**, 343 (1959).
- ⁹ H. de Raedt and Ad Lagendijk, Phys. Rev. B **27**, 6097 (1983); **30**, 1671 (1984).
- ¹⁰ P. E. Kornilovitch, Phys. Rev. Lett. **81**, 5382 (1998).
- ¹¹ E. de Mello and J. Ranninger, Phys. Rev. B **55**, 14872 (1997); A. S. Alexandrov, V. V. Kabanov, and D. K. Ray, *ibid.* **49**, 9915 (1994); G. Wellein and H. Fehske, *ibid.* **56**, 4513 (1997).
- ¹² M. Capone, W. Stephan, and M. Grilli, Phys. Rev. B **56**, 4484 (1997).
- ¹³ S. R. White, Phys. Rev. B **48**, 10345 (1993); E. Jeckelmann and S. R. White, *ibid.* **57**, 6376 (1998).
- ¹⁴ S. Ciuchi, F. de Pasquale, S. Fratini, and D. Feinberg, Phys. Rev. B **56**, 4494 (1997).
- ¹⁵ M. Capone, S. Ciuchi, and C. Grimaldi, Europhys. Lett. **42**, 523 (1998).
- ¹⁶ A.H. Romero, D. W. Brown, and K. Lindenberg, Phys. Rev. B **59**, 13728 (1999).
- ¹⁷ J. Bonca, S. A. Trugman, and I. Batistic, Phys. Rev. B **60**, 1633 (1999).
- ¹⁸ V. Cataudella, G. De Filippis, and G. Iadonisi, Phys. Rev. B **60**, 15163 (1999); **62**, 1496 (2000).
- ¹⁹ W. P. Su, J. R. Schrieffer, and A. J. Heeger, Phys. Rev. Lett. **42**, 1698 (1979); Phys. Rev. B **22**, 2099 (1980).
- ²⁰ Y. Lu, *Solitons and Polarons in Conducting Polymers*, World Scientific, Singapore 1988.
- ²¹ A. La Magna and R. Pucci, Phys. Rev. B **55**, 6296 (1997).
- ²² M. Zoli, Phys. Rev. B **66**, 012303 (2002); **67**, 195102 (2003).
- ²³ M. Capone and S. Ciuchi, Phys. Rev. Lett. **91** 186405 (2003).
- ²⁴ Y. Toyozawa, Prog. Theor. Phys. **26**, 29 (1961).

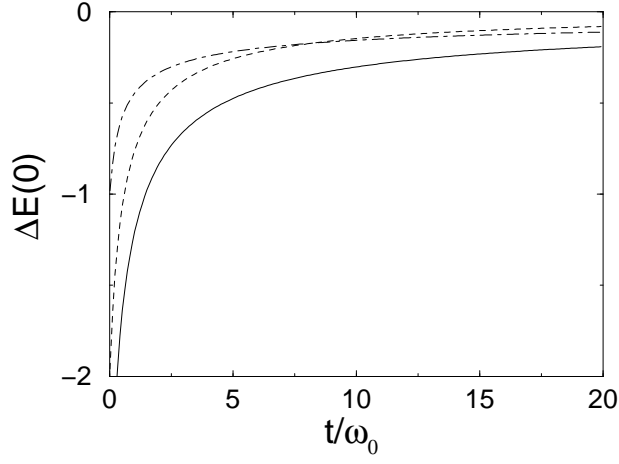


FIG. 1. Second order correction to the ground state energy, Eq. (6), as a function of the adiabatic inverse ratio \tilde{t} , for $g = g_1 = 1$ (solid line). The dashed line is the SSH-like contribution ($g = 1$ and $g_1 = 0$), the dot-dashed line is the Holstein contribution ($g = 0$ and $g_1 = 1$).

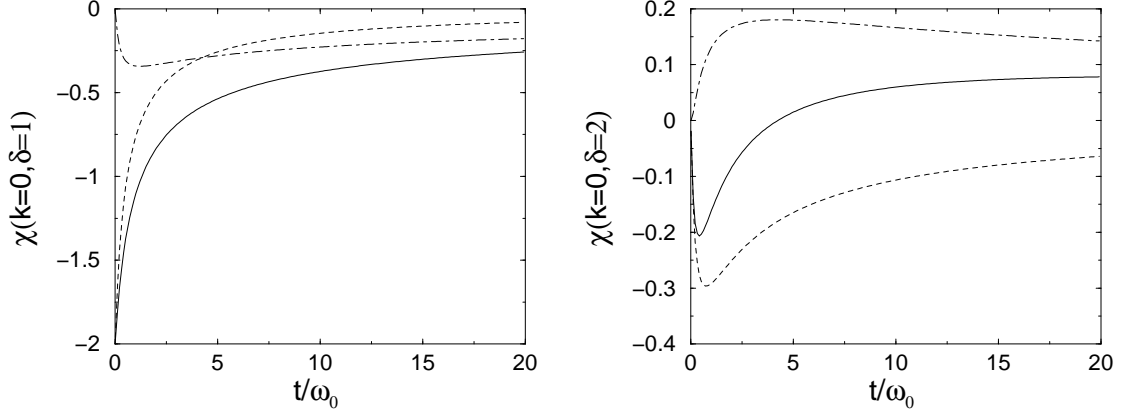


FIG. 2. Left: Correlation functions at nearest-neighbor sites (on the left) and next-nearest-neighbor sites (on the right) at $k = 0$ as functions of the inverse adiabatic ratio \tilde{t} , for $g = g_1 = 1$ (solid line). The dashed lines show the SSH-like contribution ($g = 1$ and $g_1 = 0$), the dot-dashed lines the Holstein ones ($g = 0$ and $g_1 = 1$).

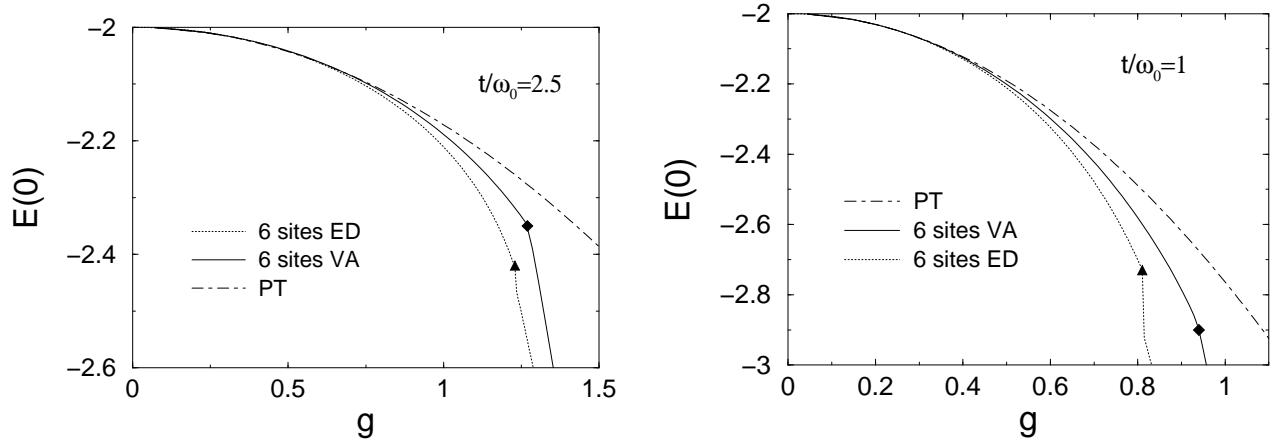


FIG. 3. Ground state energy $E(0)$ as a function of the SSH el-ph coupling g for two different values of the inverse adiabatic ratio $\tilde{t} = 2.5$ (left) and $\tilde{t} = 1$ (right). Solid and dotted lines are obtained from the variational approach and the Lanczos data for a six-site lattice, respectively; perturbative curves (dot-dashed lines) are plotted for comparison. Symbols mark the kink values of the energy.

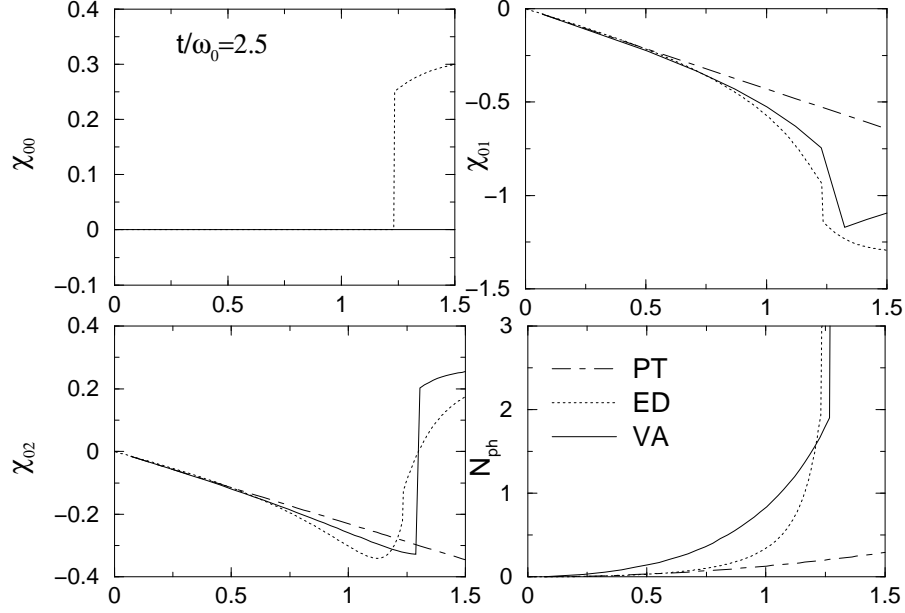


FIG. 4. Correlation functions $\chi_{k=0,\delta}$ with $\delta = 0$ (top left), $\delta = 1$ (top right) and $\delta = 2$ (bottom left) as functions of the SSH coupling g for $\tilde{t} = 2.5$. Bottom right: Phonon number vs. g for the same value of \tilde{t} . Solid lines are obtained from the variational approach in the thermodynamical limit; dotted lines show Lanczos data; perturbative curves from Eqs. (8) and Eq. (7) with $g_1 = 0$ (dot-dashed lines) are plotted for comparison.

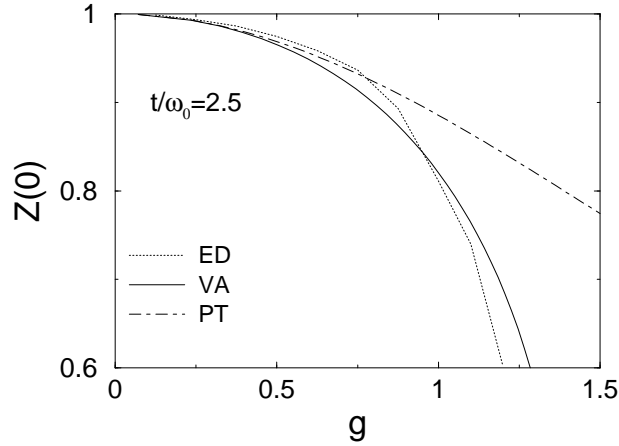


FIG. 5. Spectral weight $Z(0)$ as a function of the SSH el-ph coupling g for $\tilde{t} = 2.5$. The solid line is obtained from the variational approach in the thermodynamical limit; the dotted line shows Lanczos data; the perturbative curve from Eq. (9) with $g_1 = 0$ (dot-dashed line) is plotted for comparison.

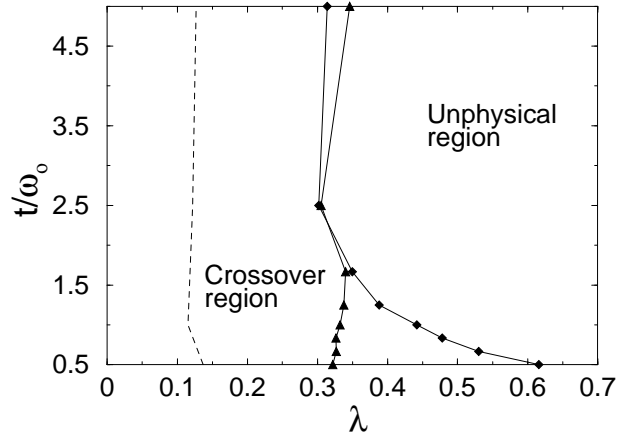


FIG. 6. Phase diagram for one electron in a six-site lattice. Triangles and diamonds correspond, respectively, to the couplings where the exact numerical ground state energy and the variational result have a kink. The dashed line indicates the boundary of the crossover region, where the spectral weight $Z(0)$ is less than 0.9.